

# **Tunnel support in weak rock**

Evert Hoek

Keynote address, *Symposium of Sedimentary Rock Engineering*,  
Taipei, Taiwan, November 20-22, 1998

## Tunnel support in weak rock

Evert Hoek

Consulting Engineer, 3034 Edgemont Boulevard, North Vancouver, British Columbia, Canada, V7R 4X1

**SYNOPSIS:** The stability of tunnels in weak rock is controlled by the ratio of the uniaxial compressive strength of the rock mass to the maximum in situ stress. This ratio provides a guide to the first estimate of support requirements to control strain to a specified level. Numerical analysis of the response of the tunnel to sequential excavation and support installation is the most reliable means of optimizing the support design. This approach to support design is illustrated by means of a number of practical examples.

### INTRODUCTION

Tunnelling in weak rock presents some special challenges to the geotechnical engineer since misjudgments in the design of support systems can lead to under-design and costly failures or over-design and high tunnelling costs. In order to understand the issues involved in the process of designing support for these tunnels, it is necessary to examine some basic concepts of how a rock mass surrounding a tunnel deforms and how the support system acts to control this deformation. Once these basic concepts have been explored, examples of practical support designs for different conditions will be considered.

### DEFORMATION OF AN ADVANCING TUNNEL

Figure 1 shows the results of a three-dimensional finite element analysis of the deformation of the rock mass surrounding a circular tunnel advancing through a weak rock mass subjected to equal stresses in all directions. The plot shows displacement vectors in the rock mass as well as the shape of the deformed tunnel profile. Figure 2 gives a graphical summary of the most important features of this analysis.

Deformation of the rock mass starts about one half a tunnel diameter ahead of the advancing face and reaches its maximum value about one and one half diameters behind the face. At the face position about one third of the total radial closure of the tunnel has already occurred and the tunnel face deforms inwards as illustrated in Figures 1 and 2. Whether or not these deformations induce stability problems in the tunnel depends upon the ratio of rock mass strength to the in situ stress level.

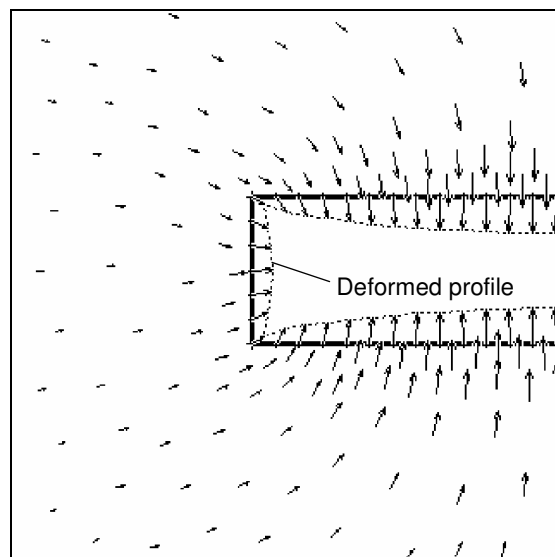


Figure 1: Vertical section through a three-dimensional finite element model of the failure and deformation of the rock mass surrounding the face of an advancing circular tunnel.

### ROCK MASS STRENGTH ESTIMATES

The properties of the rock mass used in this analysis can be estimated by means of the Hoek-Brown failure criterion (Hoek and Brown 1997). The critical rock mass parameters for this analysis are the angle of friction  $\phi$ , the cohesive strength  $c$ , the modulus of deformation  $E$  and the in situ uniaxial compressive strength  $\sigma_{cm}$ . These properties can be estimated from the Geological Strength Index  $GSI$ .

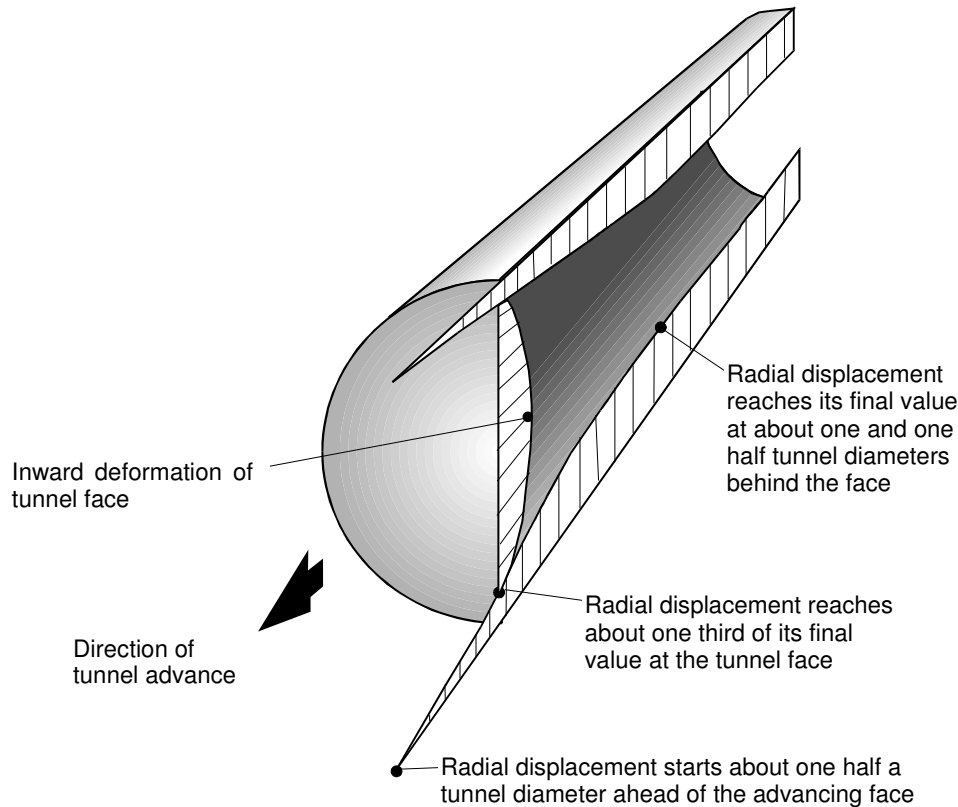


Figure 2: Pattern of deformation in the rock mass surrounding an advancing tunnel.

The value of  $GSI$  can be estimated in the field from the rock mass descriptions illustrated in Figure 3. Note that, for the purposes of this discussion on ‘weak rock masses’,  $GSI$  values from 5 to 35 are of primary interest.

For this range of values, an approximate relationship between  $GSI$  and the ratio of in situ to laboratory uniaxial compressive strengths can be derived and this is illustrated in Figure 4. This relationship provides a simple means for estimating the in situ rock mass strength  $\sigma_{cm}$  that is used in the following analysis of tunnel deformation.

#### TUNNEL DEFORMATION ANALYSIS

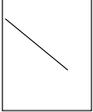
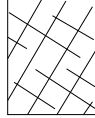
In order to explore the concepts of rock support interaction in a form which can readily be understood, a very simple analytical model can be used. This model involves a circular tunnel subjected to a hydrostatic stress field in which the horizontal and vertical stresses are equal. When the in situ stresses exceed a critical level, a zone of plastic failure develops in the rock mass surrounding the tunnel. The analysis used follows that described by Duncan-Fama (1993) and by Hoek, Kaiser and Bawden (1995).

A Monte Carlo analysis has been used to carry out this analysis for 2000 iterations for uniform distributions of the rock mass properties, tunnel radius and in situ stress level. The rock mass properties were varied from fair ( $GSI = 35$ ) to extremely poor ( $GSI = 5$ ), corresponding to the properties of weak sandstones and mudstones down to material that can almost be classed as soil. The in situ stresses ( $p_0$ ) were varied from 2 to 20 MPa, corresponding to depths below surface from 75 to 750 m, and the tunnel diameters were varied from 4 to 16 metres.

The results of this analysis are plotted in Figures 5 and 6 that give the diameter of the zone of plastic failure ( $d_p$ ) and the closure of the tunnel ( $\delta_i$ ) for different ratios of rock mass strength to in situ stress and different support pressures ( $p_i$ ).

These figures show that there is a remarkable change in the diameter of the plastic zone and the closure of the tunnel when the ratio of rock mass strength to in situ stress falls below a critical level. The role of tunnel support is to reduce this critical level.

Figure 3: Table for estimating the Geological Strength Index *GSI* of a rock mass (Hoek and Brown, 1997)

GEOLOGICAL STRENGTH INDEX		SURFACE CONDITIONS				
<p>From the description of structure and surface conditions of the rock mass, pick an appropriate box in this chart. Estimate the average value of the Geological Strength Index (GSI) from the contours. Do not attempt to be too precise. Quoting a range of GSI from 36 to 42 is more realistic than stating that GSI = 38. It is also important to recognize that the Hoek-Brown criterion should only be applied to rock masses where the size of the individual blocks or pieces is small compared with the size of the excavation under consideration. When individual block sizes are more than approximately one quarter of the excavation dimension, failure will generally be structurally controlled and the Hoek-Brown criterion should not be used.</p>						
STRUCTURE		DECREASING INTERLOCKING OF ROCK PIECES 				
	<p><b>INTACT OR MASSIVE</b> – intact rock specimens or massive in situ rock with very few widely spaced discontinuities</p>					
	<p><b>BLOCKY</b> - very well interlocked undisturbed rock mass consisting of cubical blocks formed by three orthogonal discontinuity sets</p>	80	70	60	N/A	N/A
	<p><b>VERY BLOCKY</b> - interlocked, partially disturbed rock mass with multifaceted angular blocks formed by four or more discontinuity sets</p>	70	60	50	N/A	N/A
	<p><b>BLOCKY/DISTURBED</b> - folded and/or faulted with angular blocks formed by many intersecting discontinuity sets</p>	60	50	40	N/A	N/A
	<p><b>DISINTEGRATED</b> - poorly interlocked, heavily broken rock mass with a mixture of angular and rounded rock pieces</p>	50	40	30	N/A	N/A
	<p><b>FOLIATED/LAMINATED</b> – Folded and tectonically sheared foliated rocks. Schistosity prevails over any other discontinuity set, resulting in complete lack of blockiness</p>	N/A	N/A	20	10	5

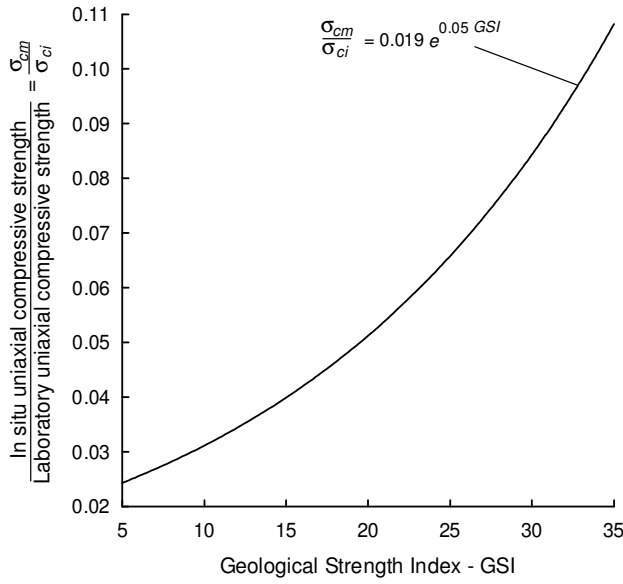


Figure 4: Approximate relationship between the Geological Strength Index (*GSI*) and the ratio of in situ to laboratory uniaxial compressive strength of the rock.

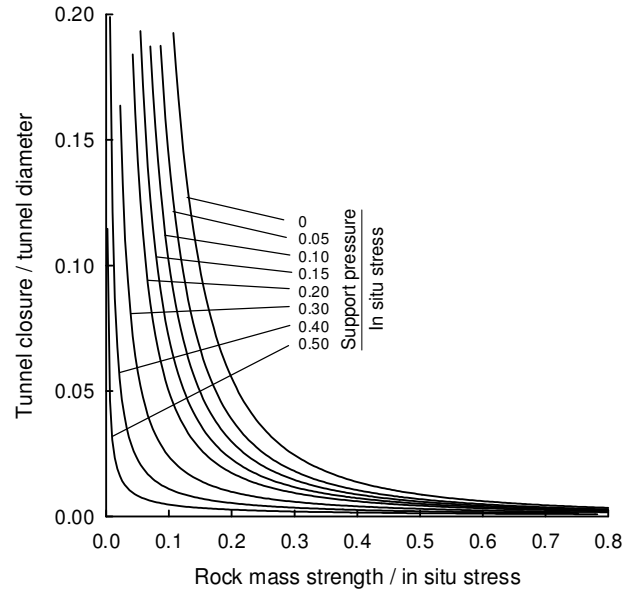


Figure 6: Tunnel deformation versus support pressure.

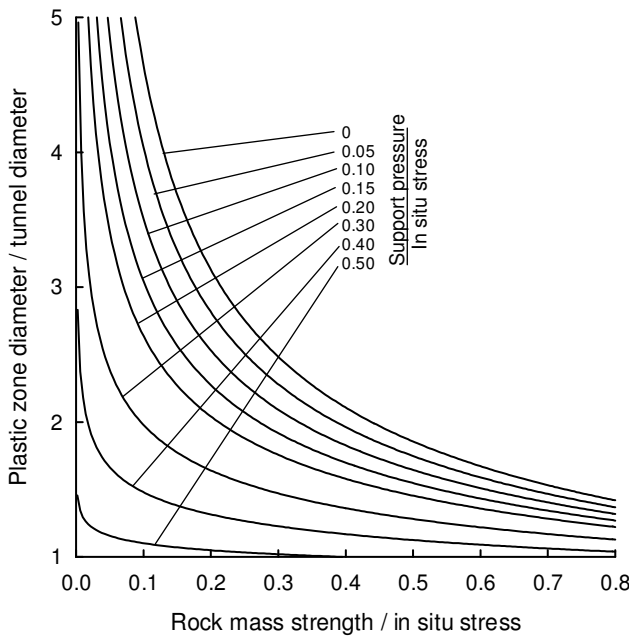


Figure 5: Size of plastic zone versus support pressure.

The curves plotted in Figures 5 and 6 are defined by the equations:

$$\frac{d_p}{d_o} = \left( 1.25 - 0.625 \frac{p_i}{p_o} \right) \frac{\sigma_{cm}}{p_o} \left( \frac{p_i}{p_o} \right)^{-0.57} \quad (1)$$

$$\frac{\delta_i}{d_o} = \left( 0.002 - 0.0025 \frac{p_i}{p_o} \right) \frac{\sigma_{cm}}{p_o} \left( \frac{2.4 \frac{p_i}{p_o} - 2}{p_o} \right) \quad (2)$$

$d_p$  = Plastic zone radius

$\delta_i$  = Tunnel sidewall deformation

$d_o$  = Original tunnel radius in metres

$p_i$  = Internal support pressure

$p_o$  = In situ stress = depth  $\times$  unit weight of rock mass

$\sigma_{cm}$  = Rock mass strength =  $2c \cos \phi / (1 - \sin \phi)$

#### CRITICAL STRAIN

Sakurai (1983) has suggested that the stability of tunnels can be assessed on the basis of the strain in the rock mass surrounding the tunnel. The maximum strain is defined by the ratio of tunnel closure ( $\delta_i$ ) to tunnel diameter ( $d_o$ ). Sakurai found that the percentage strain can be expressed by means of an equation of the form  $\epsilon_{pc} = A\sigma_{cm}^B$  where  $\sigma_{cm}$  is the rock mass strength and  $A$  and  $B$  are constants.

The application of this concept to practical tunnel problems is illustrated in Figure 7 which shows the percentage strain observed during the construction of three tunnels in Taiwan<sup>1</sup>. It can be seen that those tunnels categorized as requiring special support consideration fall above a line that is well defined by Sakurai's critical strain concept.

Note that this critical strain only defines the boundary between those tunnels that do not require special consideration and those that need careful consideration in terms of support design. In fact, all of the tunnels included in Figure 7 were constructed successfully, including those that suffered strains of approximately 10%. In some of these cases the tunnels had to be re-mined since the profiles were no longer adequate to accommodate the service structures for which they were designed.

The idea of using strain as a basis for tunnel design can be taken a step further by considering the amount of support required to limit the strain to a specified level. These support pressures can be estimated from equation 2 for the case of a circular tunnel and are plotted in Figure 8, which is a presentation of Figure 6 in a more useful form for design purposes.

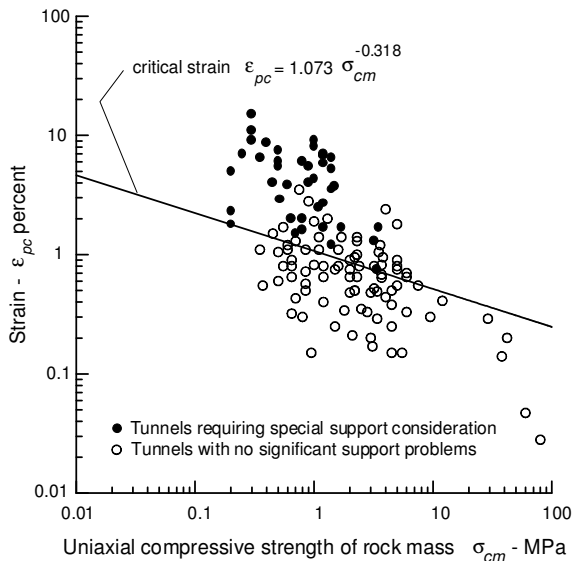


Figure 7: Percentage strain for different rock mass strengths. The points plotted are for the Second Freeway, the Pinglin and the New Tienlun Headrace tunnels in Taiwan.

<sup>1</sup> Information in this plot was supplied by Dr J.C. Chern of Sinotech Engineering Consultants Inc., Taipei.

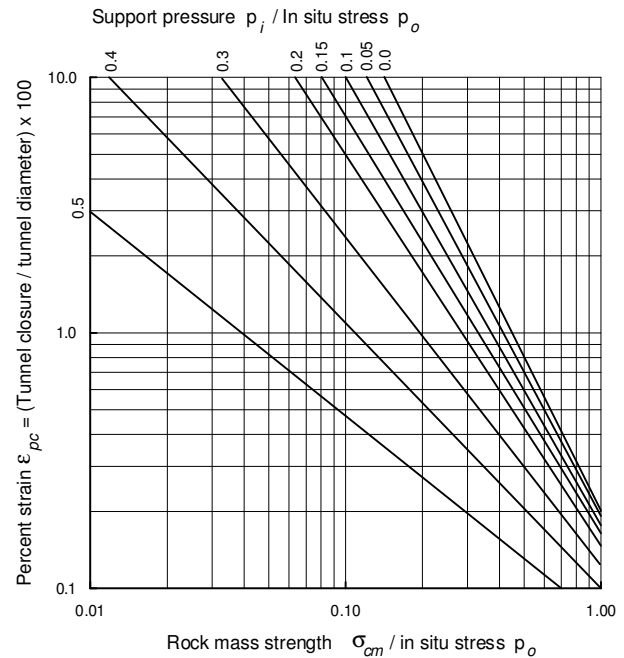


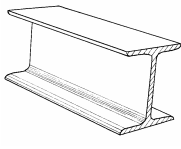
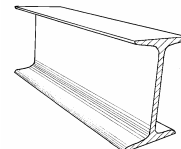
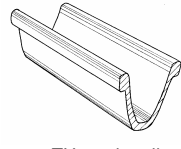
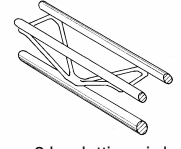
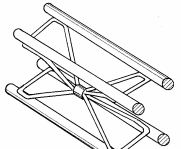
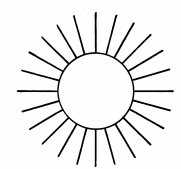
Figure 8: Approximate support pressure required for different strain values for a circular tunnel subjected to hydrostatic in situ stresses.

Note that this plot applies to a circular tunnel in a rock mass subjected to hydrostatic in situ stresses. However, it can be used to obtain an approximate first estimate of the support pressure required to limit the strain in the rock mass surrounding a tunnel. The use of this plot will be illustrated in some practical examples discussed later.

#### ESTIMATES OF SUPPORT CAPACITY

Hoek and Brown (1980) and Brady and Brown (1985) have published equations that can be used to calculate the capacity of mechanically anchored rockbolts, shotcrete or concrete linings or steel sets for a circular tunnel.

Typical support pressures for a variety of different systems for a range of tunnel sizes are plotted in Figure 9. Once again it must be emphasised that these support pressures are derived from idealised calculations for a circular tunnel and that great care has to be used in applying these values to actual problems. As illustrated in the practical examples presented later, these support estimates provide a useful starting point in a tunnel support design evaluation, but it is necessary to check the details of this design by numerical analysis.

Support type	Flange width - mm	Section depth - mm	Weight - kg/m	Curve number	Maximum support pressure $p_{i\max}$ (MPa) for a tunnel of diameter $D$ (metres) and a set spacing of $s$ (metres)
 Wide flange rib	305	305	97	1	$p_{i\max} = 19.9D^{-1.23}/s$
	203	203	67	2	$p_{i\max} = 13.2D^{-1.3}/s$
	150	150	32	3	$p_{i\max} = 7.0D^{-1.4}/s$
 I section rib	203	254	82	4	$p_{i\max} = 17.6D^{-1.29}/s$
	152	203	52	5	$p_{i\max} = 11.1D^{-1.33}/s$
 TH section rib	171	138	38	6	$p_{i\max} = 15.5D^{-1.24}/s$
	124	108	21	7	$p_{i\max} = 8.8D^{-1.27}/s$
 3 bar lattice girder	220	190	19	8	$p_{i\max} = 8.6D^{-1.03}/s$
	140	130	18		
 4 bar lattice girder	220	280	29	9	$p_{i\max} = 18.3D^{-1.02}/s$
	140	200	26		
 Rockbolts or cables spaced on a grid of $s \times s$ metres	34 mm rockbolt			10	$p_{i\max} = 0.354/s^2$
	25 mm rockbolt			11	$p_{i\max} = 0.267/s^2$
	19 mm rockbolt			12	$p_{i\max} = 0.184/s^2$
	17 mm rockbolt			13	$p_{i\max} = 0.10/s^2$
	SS39 Split set			14	$p_{i\max} = 0.05/s^2$
	EXX Swellex			15	$p_{i\max} = 0.11/s^2$
	20mm rebar			16	$p_{i\max} = 0.17/s^2$
	22mm fibreglass			17	$p_{i\max} = 0.26/s^2$
	Plain cable			18	$p_{i\max} = 0.15/s^2$
	Birdcage cable			19	$p_{i\max} = 0.30/s^2$

Support type	Thickness - mm	Age - days	UCS - MPa	Curve number	Maximum support pressure $p_{i\max}$ (MPa) for a tunnel of diameter $D$ (metres)
 Concrete or shotcrete lining	1m	28	35	20	$p_{i\max} = 57.8D^{-0.92}$
	300	28	35	21	$p_{i\max} = 19.1D^{-0.92}$
	150	28	35	22	$p_{i\max} = 10.6D^{-0.97}$
	100	28	35	23	$p_{i\max} = 7.3D^{-0.98}$
	50	28	35	24	$p_{i\max} = 3.8D^{-0.99}$
	50	3	11	25	$p_{i\max} = 1.1D^{-0.97}$
	50	0.5	6	26	$p_{i\max} = 0.6D^{-1.0}$

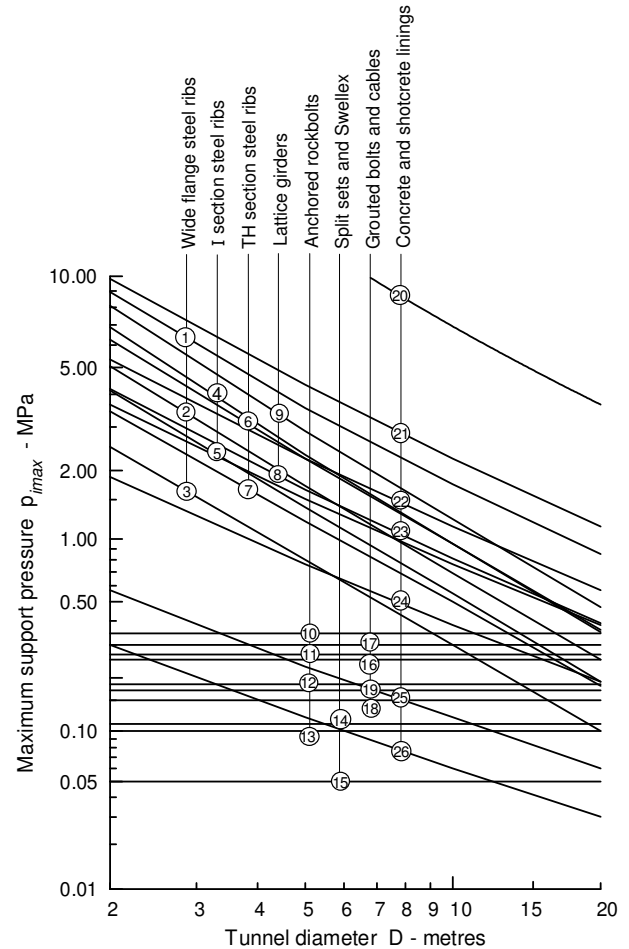


Figure 9: Approximate maximum capacities for different support systems installed in circular tunnels. Note that steel sets and rockbolts are all spaced at 1 m.

Note that all of the support pressures in Figure 9 have been plotted for steel set or rockbolt spacings of 1 m and that, in order to determine the support pressures for other spacings, the equations given for each support type should be used.

When support types are combined, the total available support pressure can be estimated by summing the maximum allowable pressures for each system. However, in making this assumption it has to be realised that these support systems do not necessarily act at the same time and that it may be necessary to check the compatibility of the systems in terms of deformation. For example if steel sets embedded in shotcrete are installed immediately behind the tunnel face, the steel sets will accept load immediately while the shotcrete will accept an increasing amount of load as it hardens (compare curves 24, 25 and 26 in Figure 9). Depending on the rate of advance of the tunnel, it may be necessary to check that the capacity of the steel sets is not exceeded before the shotcrete has hardened to the extent that it can carry its full share of the load.

#### PRACTICAL EXAMPLE OF SUPPORT DESIGN

In order to demonstrate the application of the concepts presented earlier and the extension of these concepts by the use of numerical analysis, a practical tunnel design problem is considered. The problem involves a 10 m span modified horseshoe-shaped tunnel driven through very poor quality rock at an increasing depth as it penetrates a mountain range. It is assumed that the rock mass properties and the ratio of the in situ stresses remain constant. The horizontal stress is assumed to be 1.3 times the vertical stress. The stability of the tunnel is examined at depths below surface of 50, 250 and 500 m.

The rock mass is a graphitic phyllite with a uniaxial compressive strength, determined by laboratory tests, of  $\sigma_{ci} = 15$  MPa. The rock mass is described as ‘disintegrated’, consisting of a poorly interlocked mixture of angular and rounded pieces, and ‘poor’ with slickensided and highly weathered surfaces. From Table 3, these descriptions give an approximate Geological Strength Index  $GSI = 25$ . From Figure 4, the uniaxial compressive strength of the rock mass is estimated as  $\sigma_{cm} = 1$  MPa.

#### Empirical analysis

The preliminary analysis of tunnel deformation and required support is carried out in the sequence presented in Table 1. This involves estimating the in situ stresses and the ratio of rock mass strength to in situ stress for each of

the tunnel depths. The strain for each tunnel is then estimated from equation 2.

Table 1: Support estimation sequence

Depth below surface - m	50	250	500
Vertical in situ stress $p_o$ - MPa	1.25	6.25	12.5
Strength to stress ratio - $\sigma_{cm}/p_o$	0.8	0.16	0.08
Strain without support - % (eqn. 2)	0.3	7.8	31.3
$p_i/p_o$ for 2 % strain (Figure 8)	0	0.25	0.35
$p_i$ for 2 % strain – MPa	0	1.6	4.4
$p_i/p_o$ for 5 % strain (Figure 8)	0	0.1	0.24
$p_i$ for 5 % strain - MPa	0	0.63	3.0

For the 50 m deep tunnel with no support, the strain is only 0.3 % and hence no major support requirements are anticipated. For the 250 m deep tunnel with no support, the strain of 7.8% suggests that significant stability problems will occur unless adequate support is provided. For the 500 m deep tunnel with no support, the strain of more than 30% will probably result in collapse of the tunnel. Special consideration of the support requirements will be required for this case.

The support required to limit strain to 2% and 5% has been estimated for each of the tunnels in Table 1.

In the case of the 250 m deep tunnel, the support pressure of 1.6 MPa for 2 % strain is not difficult to achieve for a 10 m span tunnel with a combination of two support elements. For example, three-bar lattice girders, spaced at 1 m, embedded in a 150mm thick shotcrete layer (curves 8 and 22 in Figure 9) will give a support pressure of approximately 1.8 MPa. Alternatively, a 1 m x 1 m pattern of 34 mm diameter rockbolts together with a 200 mm thick shotcrete lining (curves 10 and interpolating between curves 21 and 22 in Figure 9) will give the required support pressure of 1.6 MPa.

Note that, when using rockbolts, the size of the plastic zone surrounding the tunnel should be checked and the bolts should extend 1.5 to 2 m beyond this zone to ensure that they are anchored in undamaged rock. This can be done by substituting the appropriate values for the ratios  $\sigma_{cm}/p_o = 0.16$  and  $p_i/p_o = 0.25$  in equation 1. The plastic zone is approximately twice the diameter of the tunnel. Hence the thickness of the plastic zone is approximately 5 m. Consequently, the rockbolts should be 6.5 to 7 m long.

For the 500 m deep tunnel, the support pressures of 4.4 MPa for 2% strain and 3 MPa for 5% strain are difficult to achieve without resorting to very heavy steel ribs embedded in shotcrete or concrete. It may be necessary

to add yielding elements to the ribs and to use forepoling to stabilise the face. These support measures are discussed in detail in the following section.

### Finite element analysis

The empirical analysis described above is useful for determining whether or not a tunnel will require significant support. It can also be used to obtain a first estimate of the support pressure required to limit the size of the plastic zone or the closure of the tunnel. However, for most practical cases, these estimates are not adequate and it is necessary to carry out a numerical analysis of the rock-support interaction.

Several commercial numerical programs are suitable for this type of analysis and two of the best known are FLAC<sup>2</sup>, a very powerful finite difference program, and PHASE2<sup>3</sup> a simpler but more user friendly finite element program. For the analysis presented below, the program PHASE2 was used.

The input data required for a numerical analysis is more comprehensive than that required for the empirical analysis described earlier. The parameters required can be estimated by means of the methods described by Hoek and Brown (1997). A detailed discussion on the derivation of these parameters exceeds the scope of this paper but the input data is summarized in Table 2.

The horizontal in situ stress, as defined earlier, is 1.3 times the vertical stress due to the weight of the overburden. It is assumed that the rock mass failure characteristics are elastic-perfectly plastic and that no volume change occurs at failure. Hence, the peak and residual strength parameters are the same and the dilation angle  $\alpha$ , used by the program PHASE2, is equal to zero.

The results of a series of finite element analyses, for the tunnel at depths of 50, 250 and 500 m below surface, are illustrated in Figures 10, 11 and 12. These show the size of the plastic failure zone (denoted by the  $\times$  symbols, for shear failure, and the  $\bullet$  symbols, for tensile failure) and also the shape of the deformed tunnel boundary. Note that, because the tunnel is not circular and because the in situ stress field is asymmetrical, the shapes of the plastic zones and the deformed boundaries are asymmetrical.

<sup>2</sup> Available from the ITASCA Consulting Group Inc., Thresher Square East, 708 South Third Street, Suite 310, Minneapolis, Minnesota 55415, USA, Fax + 1 612 371 4717. Internet: <http://www.itascacg.com>.

<sup>3</sup> Available from Rocscience Inc., 31 Balsam Avenue, Toronto, Ontario, Canada M4E 3B5, Fax + 1 416 698 0908. Internet: <http://www.rocscience.com>.

Table 2: Input parameters for finite element analysis

Intact rock strength $\sigma_{ci}$	15 MPa
Hoek-Brown constant $m_i$	10
Geological Strength Index $GSI$	25
Rock mass friction angle $\phi$	24.7°
Rock mass cohesion $c$	0.33 MPa
Rock mass deformation modulus	913 MPa

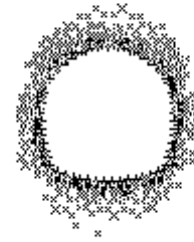


Figure 10: Plastic zone size and tunnel closure for a depth of 50 m below surface. Horizontal span of plastic zone = 13.2 m, vertical span of plastic zone = 16.1 m, horizontal strain = 0.3%, vertical strain = 0.33%.

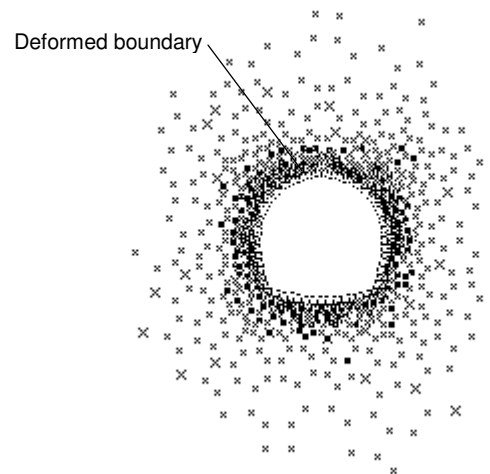


Figure 11: Plastic zone size and tunnel closure for a depth of 250 m below surface. Horizontal span of plastic zone = 27.2 m, vertical span of plastic zone = 33.5 m, horizontal strain = 5%, vertical strain = 5.3%.

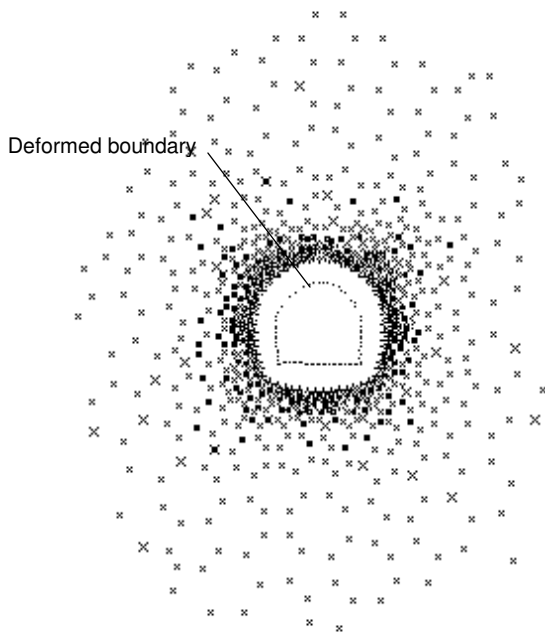


Figure 12: Plastic zone size and tunnel closure for a depth of 500 m below surface. Horizontal span of plastic zone = 35 m, vertical span of plastic zone = 45 m, horizontal strain = 15%, vertical strain = 16%.

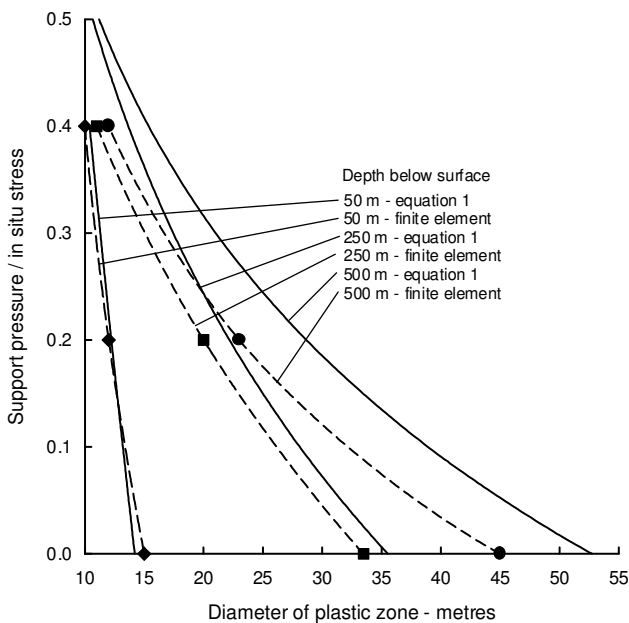


Figure 13: Plastic zone sizes predicted by equation 1 and by finite element analysis.

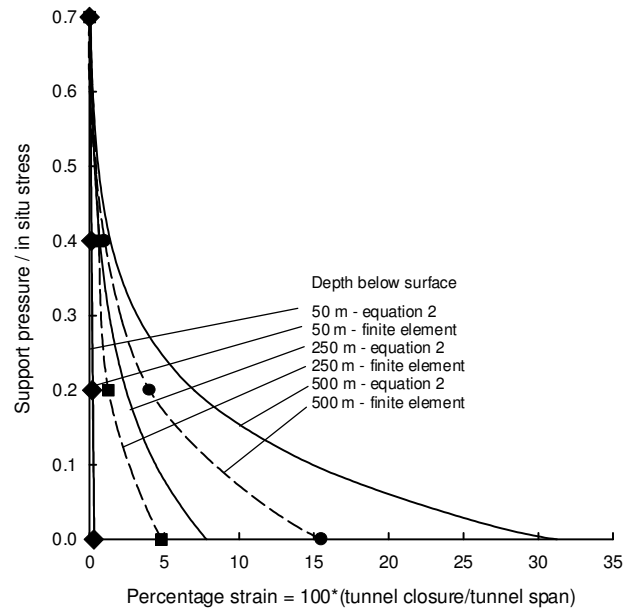


Figure 14: Percentage strain predicted by equation 2 and by finite element analysis.

Comparisons between the size of the plastic zone and the percentage strain, for different ratios of support pressure to in situ stress, are plotted in Figures 11 and 12. Note that the empirical relationships (equations 1 and 2) tend to over-predict the extent of the failure zone and the tunnel boundary deformation for these tunnels. This is because the constants used in the empirical equations have been deliberately chosen on the conservative side. This has been done in order to avoid over-optimistic predictions that could lead the user to conclude that there are no support requirements when, in fact, there may be a significant amount of rock mass failure.

Figure 10 shows that, in spite of the fact that the strain is only about 0.3%, the thickness of the plastic zone in the roof of the tunnel is approximately 3 m. In the interests of safety, it would be prudent to install a light pattern of rockbolts and a layer of shotcrete in the roof of the tunnel. Typically, a 2 m x 2 m pattern of 5 m long, 25 mm diameter rockbolts and a 50 mm layer of shotcrete will be sufficient to protect workers and equipment from small roof falls.

The extent of rock mass failure and of tunnel deformation for the 250 m deep tunnel is such that a significant amount of support is required. As shown in Table 1, a support pressure of approximately 1.6 MPa will reduce the strain to about 2%. Equation 1 predicts that, for these conditions, the diameter of the plastic zone is about 20 m, giving a thickness of the plastic zone of 5 m.

A finite element analysis of this case, with a 1 m x 1 m pattern of 5 m long, 34 mm diameter, untensioned, fully grouted rockbolts and a 200 mm thick layer of shotcrete, gives the results presented in Figure 15.

In order to simulate the three-dimensional effects of the tunnel advance, the analysis was carried out in three stages.

In stage 1, the model, without the tunnel excavated or the support installed, was allowed to consolidate under the in situ stress field.

In stage 2, the tunnel was excavated and a uniform internal support pressure of 1.6 MPa was applied to the internal boundary of the tunnel. This pressure was chosen to limit the closure of the tunnel to about 0.2 m or 2%. This is about 30% of the total closure of 0.78 m or 7.8% that is the maximum strain predicted by equation 2. As illustrated in Figure 2, this amount of deformation will already have taken place before the support can be installed, assuming that this support is installed immediately behind the advancing face.

In stage 3 the internal pressure was removed, simulating the reduction of support due to the advance of the tunnel face, and the rockbolts and shotcrete were installed.

A detailed examination of the results of this analysis showed that a closure of 0.14 m (1.4%) occurred during stage 2 and that this increased to 0.16 m (1.6%) during stage 3. A limited amount of yield was found in some of the rockbolts near the tunnel boundary. This yield is to be expected and it does not detract from the effectiveness of the rockbolts, provided that an un-yielded anchor length of 1.5 to 2 m remains in the undisturbed rock mass outside the plastic zone. Note that the thickness of the plastic zone, shown in Figure 15, is about 3 m.

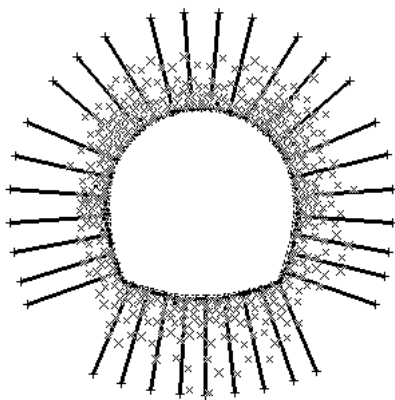


Figure 15: Plastic zone formation in a tunnel at a depth of 250 m, supported by rockbolts and shotcrete.

Figure 12 shows that, for a tunnel at a depth of 500 m, the plastic zone is very large and that the closure of the tunnel is of the order of 1.5 m. For tunnels exhibiting this degree of squeezing, experience shows that it is very difficult to provide support using conventional systems. Very heavy steel ribs or a thick concrete lining would be needed in order to provide the required support pressure but it is practically impossible to install these safely in an advancing tunnel. Consequently, support systems that can accommodate large amounts of displacement have to be considered and, if necessary, the tunnel has to be excavated over-size in order to accommodate these systems.

One method that has been used successfully in such circumstances is the 'umbrella arch' system described by Carrieri et al (1991) and Grasso et al (1993). This consists of a series of overlapping forepoles which, for a tunnel of this size, would be 12 m long, 75 mm diameter grouted pipes. These forepoles would be installed at a spacing of 8 m along the tunnel to allow a 4 m overlap between successive arches. Where necessary, fibreglass dowels can be grouted into the face of the tunnel in order to control deformation and failure of the rock mass immediately ahead of the face. A full discussion of this support system is included in the papers mentioned above and in a comprehensive discussion on tunnel support in weak rock in notes published by the author on the Internet site <http://www.rocscience.com>.

An alternative support method that can be used for very heavy squeezing conditions is one that includes yielding elements in the steel ribs. A typical yielding element is illustrated in Figure 16 that shows two Toussaint-Heintzmann (also known as 'Top Hat') profile steel ribs nested together and clamped to form a frictional sliding joint. Two or three of these yielding elements are incorporated in each steel rib and they are set to slide a pre-determined distance, depending upon the amount of closure to be allowed, before encountering a positive stop welded onto the rib.

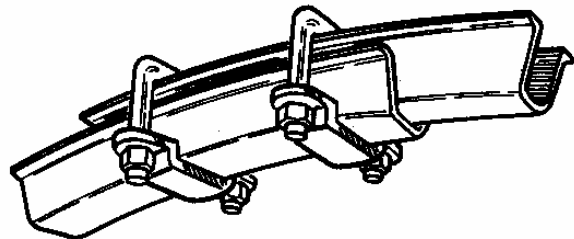


Figure 16: Assembly of a sliding joint in a Toussaint-Heintzmann or Top Hat section steel rib.

As shown in Figure 9, 124 mm x 108 mm T-H section steel rib at a 1 m spacing will provide a support pressure of approximately 0.5 MPa and, if this is embedded in a 150 mm thick shotcrete lining, the total support capacity is approximately 1.6 MPa.

A finite element analysis of this case is carried out in three stages. As in the previous example, the first stage is a consolidation stage in which the model, with no excavation present, is allowed to deform while being loaded by the in situ stress field.

In the second stage, after excavation of the tunnel, a uniform support pressure (normal traction) is applied to the tunnel boundary to control the closure of the tunnel. As shown in Figure 2, the initial closure that occurs before the ribs are installed is assumed to be one third of the total closure. For this case this initial closure is approximately 0.5 m or 5%. Assuming that two yielding elements are installed and that each is allowed to slip 0.3 m before locking up, a further 2% closure will take place before the ribs and the shotcrete lining are required to carry the residual load. From Figure 14, the support pressure required to control the total closure to 7% is approximately  $0.1 \times 12.5 = 1.25$  MPa.

In the third stage, the internal support pressure of 1.25 MPa is removed and a composite lining is installed to represent the combined support provided by the T-H ribs embedded in a 150 mm thick shotcrete layer. This composite lining is constructed by increasing the strength and stiffness of a 150 mm thick lining to simulate the coupled behaviour of the ribs and the shotcrete (see Brady and Brown 1985). In this case, the 150 mm thick lining has been assigned a deformation modulus of 35,000 MPa, a compressive strength of 42.5 MPa and a tensile strength of 30 MPa. The results of the finite element analysis, illustrated in Figure 17, show that the final tunnel closure was approximately 7.5%. The horizontal span of the plastic zone was 23 m and the vertical span 28 m (compare with Figure 12 for the unsupported tunnel).

In this analysis, a certain amount of trial and error is usually required to balance the amount of deformation that should be allowed in the yielding elements and the final load carried by the ribs and shotcrete. Too little deformation in the yielding elements will result in too high a residual load that has to be carried by the ribs and shotcrete. This can give rise to buckling of the steel ribs and cracking of the shotcrete lining. Too much deformation in the yielding elements will result in excessive closure of the tunnel and, possibly, in the rock mass surrounding the tunnel breaking up as it deforms.

These signs are very obvious in the field and they can be used to optimise the amount of deformation of the yielding elements.

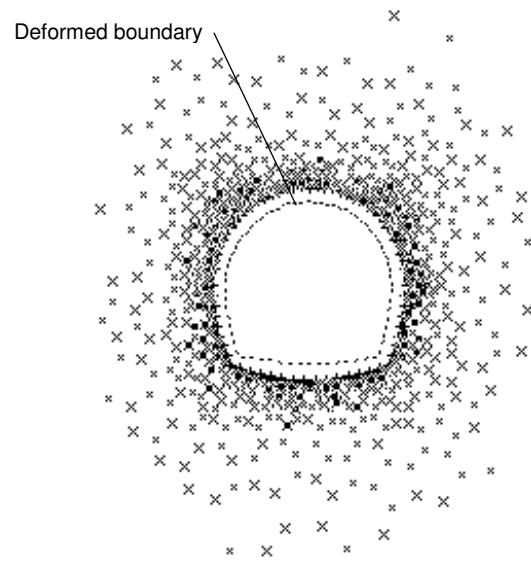


Figure 17: Plastic zone size and deformed boundary for the tunnel at a depth of 500 m below surface with support provided by T-H section steel ribs, with yielding elements, embedded in shotcrete.

Sánchez and Terán (1994) describe the use of yielding elements in steel ribs for the support of the Yacambú-Quibor tunnel in Venezuela – regarded by many as one of the most difficult tunnels in the world. This 5.5 m diameter water supply tunnel through the Andes is being excavated through weak rock masses, including graphitic phyllites, at a maximum depth below surface of 1200 m. In the weakest rock sections, the support consists of WF6x20 steel ribs, at 1 m spacing, with two sliding joints. These joints are set to lock when an additional tunnel closure of about 300 mm has been achieved. The ribs are installed immediately behind the tunnel face and they are embedded in shotcrete, except for a 1 m wide ‘window’ that is left for each of the sliding joints. Once the joints have moved and locked, usually between 5 a 10 m behind the face, the ‘windows’ are closed to complete the shotcrete lining. This support system has proved to be very effective and measurements of tunnel convergence, carried out over several years, have shown that the tunnel is completely stable.

## CONCLUSION

The design of support for tunnels in weak rock is a complex problem. In some cases the apparently logical approach of installing more and heavier support to resist the squeezing pressures is, in fact, the wrong approach. Flexible support systems, with the use of forepole um-

brellas or of yielding elements where required, will usually result in a support system that is both effective and economical.

It has not been possible to explore all of the options available to the weak rock tunnel designer. Many of the concepts outlined in this paper have not been fully developed and, in some cases, better alternatives may be found. There are ample opportunities, for those interested in rock engineering research, to carry these ideas further and to develop a logical methodology for tunnel support design in weak rock masses.

## REFERENCES

- Brady, B.H.G. and Brown, E.T. (1985). *Rock mechanics for underground mining*. Allen and Unwin, London.
- Carrieri, G., Grasso, P., Mahtab, A. and Pelizza, S. (1991). Ten years of experience in the use of umbrella-arch for tunnelling. *Proc. SIG Conf. On Soil and Rock Improvement, Milano 1*, 99-111.
- Duncan Fama, M.E. (1993). Numerical modelling of yield zones in weak rocks. In *Comprehensive rock engineering*, (ed. J.A. Hudson) 2, 49-75. Pergamon, Oxford.
- Grasso, P., Mahtab, M.A., Rabajoli, G. and Pelizza, S. (1993). Consideration for design of shallow tunnels. *Proc. Infrastructures souterraines de transport, Toulon*, 19-28.
- Hoek, E., and Brown, E.T. (1980). *Underground excavations in rock*. Instn Min. Metall., London.
- Hoek, E., Kaiser, P.K. and Bawden. W.F. (1995). *Support of underground excavations in hard rock*. Balkema, Rotterdam.
- Sakurai, S. (1983). Displacement measurements associated with the design of underground openings. *Proc. Int. Symp. Field Measurements in Geomechanics, Zurich 2*, 1163-1178.
- Sánchez Fernández, J.L. and Terán Benítez, C.E. (1994). Túnel de Tránsito Yacambú-Quibor. "Avance Actual de los Trabajos de Excavación Mediante la Utilización de Soportes Flexibles Aplicados a Rocas con Grandes Deformaciones". *Proc. IV Congreso Sudamericano de Mecánica de Rocas, Santiago 1*, 489-497.